

## **Thermal Infrared Optical Metrology using Quadri-Wave Lateral Shearing Interferometry**

Sabrina Velghe<sup>a</sup>, Djamel Brahmi<sup>a</sup>, William Boucher<sup>a</sup>, Benoit Wattellier<sup>a</sup>,  
Nicolas Guérineau<sup>b</sup>, Riad Haïdar<sup>b</sup>, Jérôme Primot<sup>b</sup>

<sup>a</sup>PHASICS S.A. \*, Campus de l'Ecole Polytechnique, Palaiseau 91128, France

<sup>b</sup>ONERA, Office National d'Etudes et de Recherches Aérospatiales, Palaiseau 91761

### **ABSTRACT**

We present the application of Quadri-Wave Lateral Shearing Interferometry (QWLSI), a wave front sensing technique, to characterize thermal infrared lenses for wavelengths within 8 and 14 $\mu$ m. Wave front sensing is not only a tool to quantify optical quality, but also to map the local (dust, scratches) or global possible defects. This method offers the crucial advantage that it yields an analyzed wave front without the use of a reference arm and consequent time consuming alignment. Moreover thanks to the acceptance of QWLSI to high numerical aperture beams, no additional optics is required. This makes lens characterization convenient and very fast. We particularly show the experimental characterization of single Germanium lens and finally present the characterization of complex optical imaging systems for high-performance infrared cameras. The analysis is made in conditions that are very close to the usual conditions of the camera use; that is to say, directly in the convergent beam and in polychromatic (black body) light.

**Keywords:** Infrared, Thermal Imaging, Optical Metrology, Wave Front Sensing, PSF, MTF

### **1. INTRODUCTION**

In the last years, thermal infrared imagery has known a rapid expansion due to its large applications (intelligence gathering, security issue, night vision, thermography, ...). This expansion has been accompanied by the progress of infrared detectors technology allowing the production of large scale detector array (320x256, 640x512 pixels). The increasing demand of high-performance systems is supported by the need of control systems with high sensitivity, particularly concerning the qualification of their optical parts.

For that specific issue, the wave front sensing is a particularly adequate solution. The analysis of the wave front transmitted by a lens gives not only information on its optical quality but also leads to the numerical aperture value, focal length, point spread function and modulation transfer function. At PHASICS, we develop commercial wave front sensors, named SID4, based on Quadri-Wave Lateral Shearing Interferometry. Due to its simplicity (the set-up is only constituted with a diffractive grating and a detector array), this technology is a particularly good answer to infrared optical metrology and offers cost-effective solutions.

### **2. WAVE FRONT SENSING WITH QWLSI**

#### **2.1 The Quadri-Wave Lateral Shearing Interferometry**

In the 90s, the concept of lateral shearing interferometry has been extended to more than 2 waves by Primot and coworkers [1]. This has led to the invention of multiwave lateral shearing interferometry and, in particular, to the compact quadri-wave lateral shearing interferometer (QWLSI). The principle of this technique is very simple: the wave front is divided in replicas by a diffractive optics (see Figure 1). Each replica propagates and therefore separates from the other ones. In the region where they still overlap, the interference pattern gives access to the phase difference between each couple of diffraction orders. Because they have separated and if the propagation is short enough, this phase difference is proportional to the local phase gradient within the wave-front. Consequently each couple of replica gives

---

\* [info@phasics.fr](mailto:info@phasics.fr) ; phone +33 (0)1 69 33 89 99 ; fax +33 (0)1 69 33 89 88 ; [www.phasics.com](http://www.phasics.com)

information on the gradient along one direction (which is determined by the two replicas k-vector difference). The phase gradients are recovered thanks to Fourier analysis around each carrier-frequency associated to each replica couple.

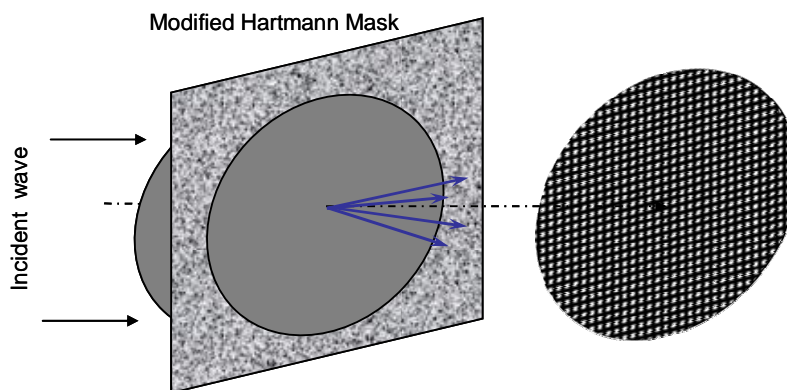


Figure 1 : Principle of Multi-Wave Lateral Shearing interferometry, illustrated in the case of four wave interference. The beam is incident from the left. It is first diffracted and interferences are recorded by a detector array.

This principle has been applied in laser metrology to 3-wave interferometers [1], which is its simplest variation. The optimization process led to 4-wave interferometers, thanks to the so-called Modified Hartmann Mask (MHM) [3]. This 2D diffractive optics has been designed to concentrate more than 90% of the power in the 4 first +/-1 diffraction orders only. It is therefore a good candidate to make a Quadri-Wave Lateral Shearing Interferometer (QWLSI).

In the case of QWLSI, the observed interference pattern is a Cartesian grid of sinusoidal fringes. If the wave front is flat, the grid pitch is the same everywhere in the pupil. If the wave front contains aberrations, the grid is deformed and the deformations are proportional to the local phase gradients. An integration process is then applied to these phase gradients in order to reconstruct the phase cartography.

## 2.2 Optical metrology with QWLSI

The characterization of lenses with QWLSI is very simple: a calibrated collimated beam propagates through the lens, the transmitted wave front is then analyzed by the QWLSI wave front sensor (see Figure 2). If the lens is perfect, the measured wave front is spherical, if not, the distance to a sphere is then the lens aberrations. From the aberration map, we can then simulate the Point Spread Function (PSF) and deduce the Modulation Transfer Function (MTF) of the lens.

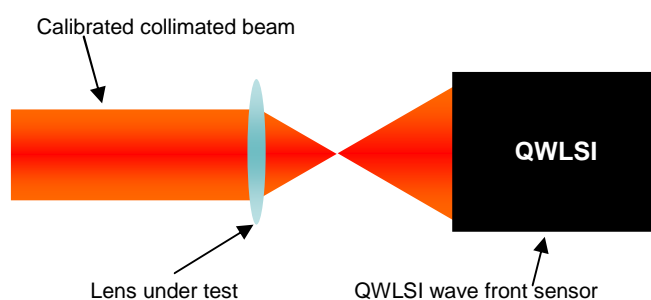


Figure 2 : Principle of lens metrology with a QWLSI.

### 3. THERMAL INFRARED OPTICAL METROLOGY

To answer the need for thermal infrared optical metrology in the long wavelength infrared (LWIR) domain ( $\lambda=8-14\mu\text{m}$ ) we developed a dedicated QWLSI, based on a particular grating and an uncooled commercial camera using a highly sensitive micro-bolometer focal plane array. This wave front sensor provides  $96\times 72$  measurement points with a spatial resolution equal to  $140\mu\text{m}$ .

#### 3.1 Experimental Set-Up

The experimental set-up is based on the principle presented on Figure 2. As a source, we used a black body (temperature  $\approx 1000^\circ\text{C}$ ) to have a polychromatic light in the LWIR domain. In order to obtain the calibrated beam, we used a collimator whose focal length is equal to 700mm. The test bench is presented on Figure 3 and the QWLSI is shown on Figure 4. We placed a pinhole between the black body and the collimator in order to provide the sufficient spatial coherence to have good contrast interference fringes (its diameter is equal to few millimeters) as shown on Figure 5. This test bench can be used to characterize single lenses and also for more complicated objectives, for cooled or uncooled cameras.

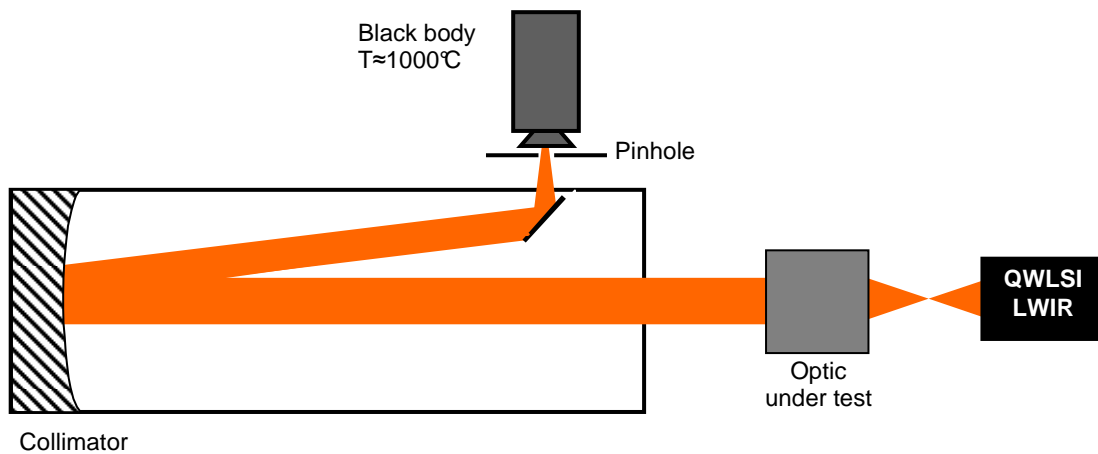


Figure 3 : Test bench for infrared metrology.

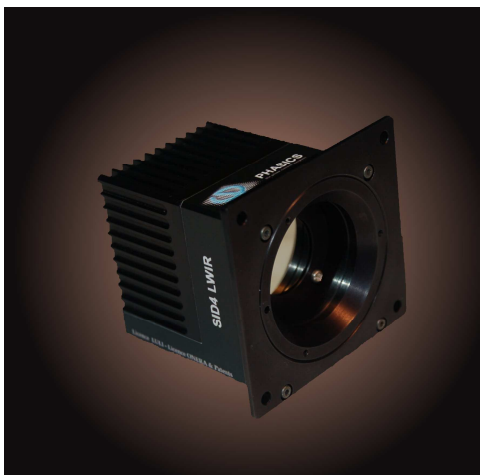


Figure 4 : The SID4-LWIR, our QWLSI for the wavelength within 8 and  $14\mu\text{m}$

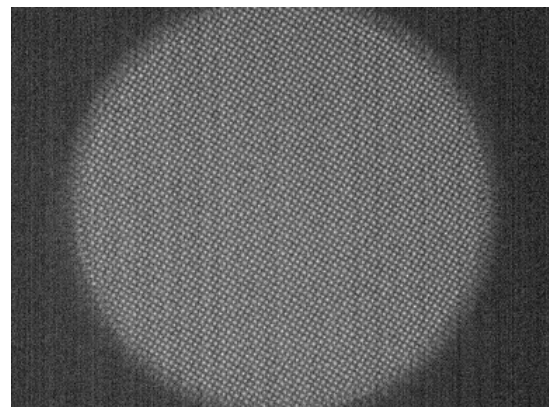
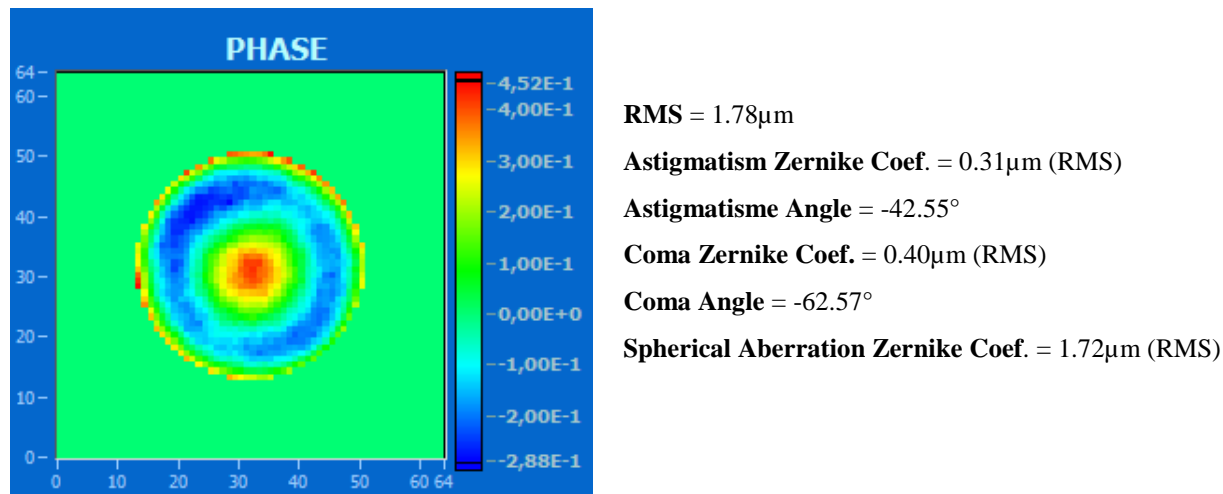


Figure 5 : Experimental interferogram obtained with a collimated beam.

### 3.2 Germanium Lens Analysis

We present here the analysis of a plano-convex Germanium lens of known characteristics (diameter=25.4mm, focal length=50.8mm, Radius of curvature= 151.01mm, Center Thickness=2.5mm). As the Germanium has very low index dispersion for wavelengths within 8 and 14 $\mu$ m, we can neglect the chromatic aberration and consider that the lens will generate the same optical path difference at all the wavelengths.

We place the plano-convex lens in the collimated beam (flat face first, in order to generate high spherical aberration) and we analyze the wave front in the divergent beam as shown on Figure 3. We use a diaphragm with a diameter equal to 22mm to limit the beam extension. The Figure 6 shows the experimental phase cartography.



(the phase is given in fraction  $\lambda$  with  $\lambda=10\mu$ m)

Figure 6 : Phase cartography obtained with the analysis of a Ge plano-convex lens.

As we analyze a plano-convex lens, the phase is mainly constituted with a spherical aberration. There is also astigmatism and coma in a lower proportion which can be due to a misalignment of the lens respectively to the collimated beam and wave front sensor.

From its specifications and the experimental conditions, we modeled the lens with an optical design software. This model gives a spherical aberration Zernike coefficient equal to 1.92 $\mu$ m RMS. This result is comparable to the experimental result (1.72 $\mu$ m). The difference can be explained by a small error on the pupil diameter used during the experiment.

From the aberration and the intensity maps, we can then simulate the Point Spread Function (PSF) and deduce the Modulation Transfer Function (MTF). Figure 7 shows the PSF and MTF obtained from the phase analysis of the Germanium lens. On the MTF figure, we plotted the horizontal and vertical MTF curves and also the MTF of an ideal lens with same numerical aperture. In this particular case, the experimental MTF is highly deteriorated compared to the theoretical one. This is directly linked to the high spherical aberration generated by a plano-convex lens, particularly when the beam is incident on the flat face of the lens. For imaging purposes, the objectives have more complex optical design and particularly use aspheric lenses in order to increase the optical properties and reach the best possible imaging quality.

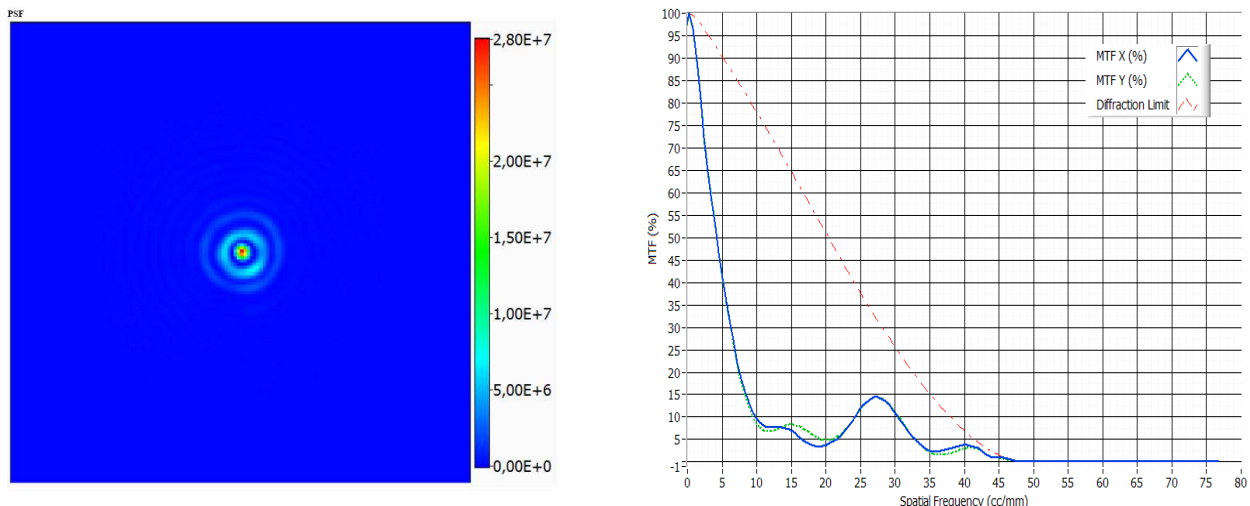


Figure 7 : Calculated PSF (on the left) and MTF (on the right) obtained from the experimental phase cartography shown on Figure 6. The horizontal (continuous line) and the vertical (dotted line) MTF curves can be compared to the diffraction limited MTF (dashed line).

### 3.3 LWIR Objective Analysis

We present here the experimental analysis of an objective used on a cooled LWIR camera. For the analysis of this type of objective, we developed a dedicated test bench allowing the analysis directly in the exit pupil of the objective [4]. This configuration has the crucial advantage that it allows the analysis on axis but also in the field. The Figure 8 shows the test bench. In this configuration, we fixed the objective under test to the QWLSI. The diffraction grating is placed in the exit pupil of the objective and, contrary to the analysis of the Ge lens presented above, we perform the analysis in the convergent beam created by the objective. The field analysis is simply obtained by rotating the assembly {Objective+QWLSI} in the collimated beam. The field angle is then the rotation angle  $\theta$ .

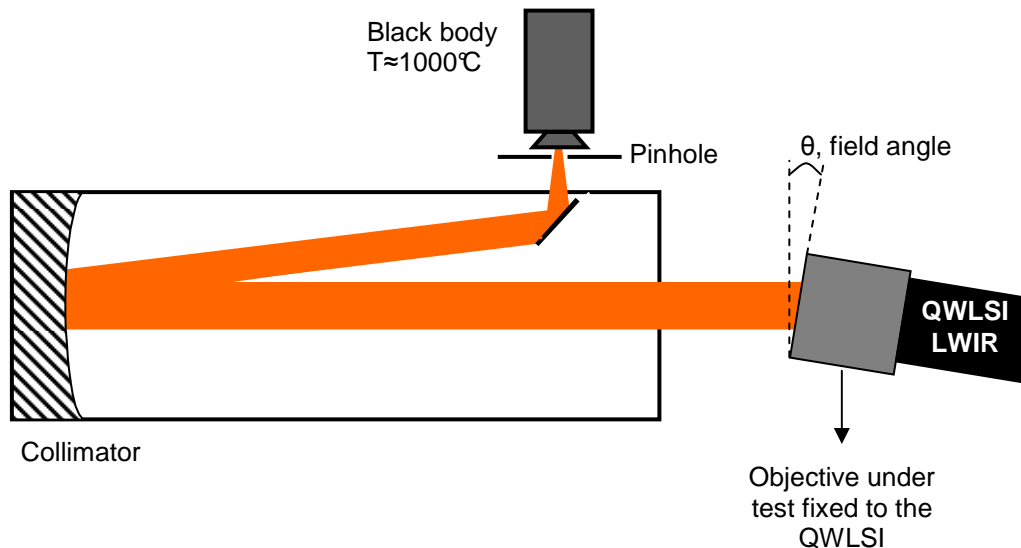
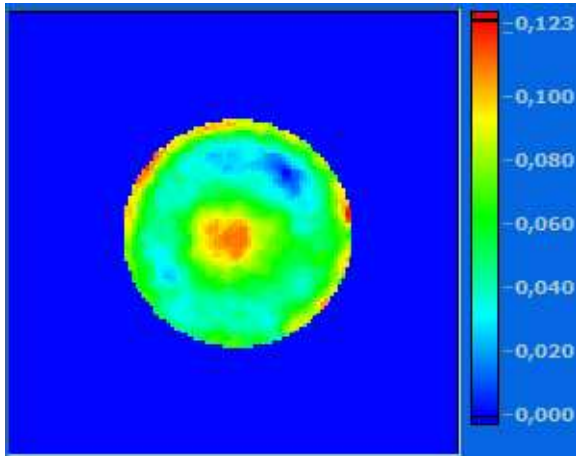


Figure 8 : Experimental test bench to analyze LWIR objectives on axis ( $\theta=0$ ) and in the field.

Figure 9 on the left shows the experimental result of the on-axis analysis. Like the analysis of the Ge plano-convex lens, the wave front is mainly constituted with a spherical aberration but the global RMS wave front error (WFE) is much smaller ( $0.22\mu\text{m}$ ). To roughly evaluate the imaging quality of this optical system, we can compare the WFE to the Maréchal Criteria [5]. This criteria indicates that a system is well corrected when its WFE is lower than  $\lambda/14$  (i.e.  $1\mu\text{m}$  at  $\lambda=14\mu\text{m}$ , the greatest wavelength of the LWIR domain) which is the case of the objective under test. This rough evaluation is confirmed by the MTF analysis. Indeed, as the wave-front is very close to a sphere, the calculated MTF curves are very similar to the theoretical MTF (see Figure 9 on the right). These results show that this objective has a high imaging quality.

### ON AXIS ANALYSIS



(the phase is given in fraction  $\lambda$  with  $\lambda=10\mu\text{m}$ )

- RMS** =  $0.22\mu\text{m}$
- Astigmatism Zernike Coef.** =  $0.065\mu\text{m}$  (RMS)
- Astigmatisme Angle** =  $-25.35^\circ$
- Coma Zernike Coef.** =  $0.074\mu\text{m}$  (RMS)
- Coma Angle** =  $-74.58^\circ$
- Spherical Aberration Zernike Coef.** =  $0.182\mu\text{m}$  (RMS)
- Analyzed Numerical Aperture** = 0.219

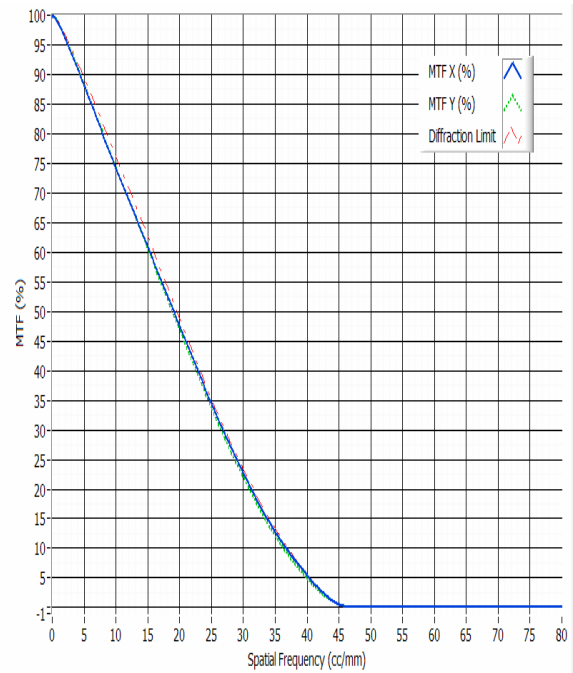


Figure 9 : On the left, experimental phase obtained by the on-axis analysis of the objective. On the right, the calculated MTF.

Figure 10 shows the experimental phase for  $\theta= \pm 9.5^\circ, \pm 5.5^\circ$  and  $\pm 1.5^\circ$ . As it should be expected, the use of the objective with increased field values progressively creates astigmatism and coma originating from spherical aberration. Moreover, the global WFEs remain small compared to the Maréchal criteria and then insure a good image quality for different field angles.

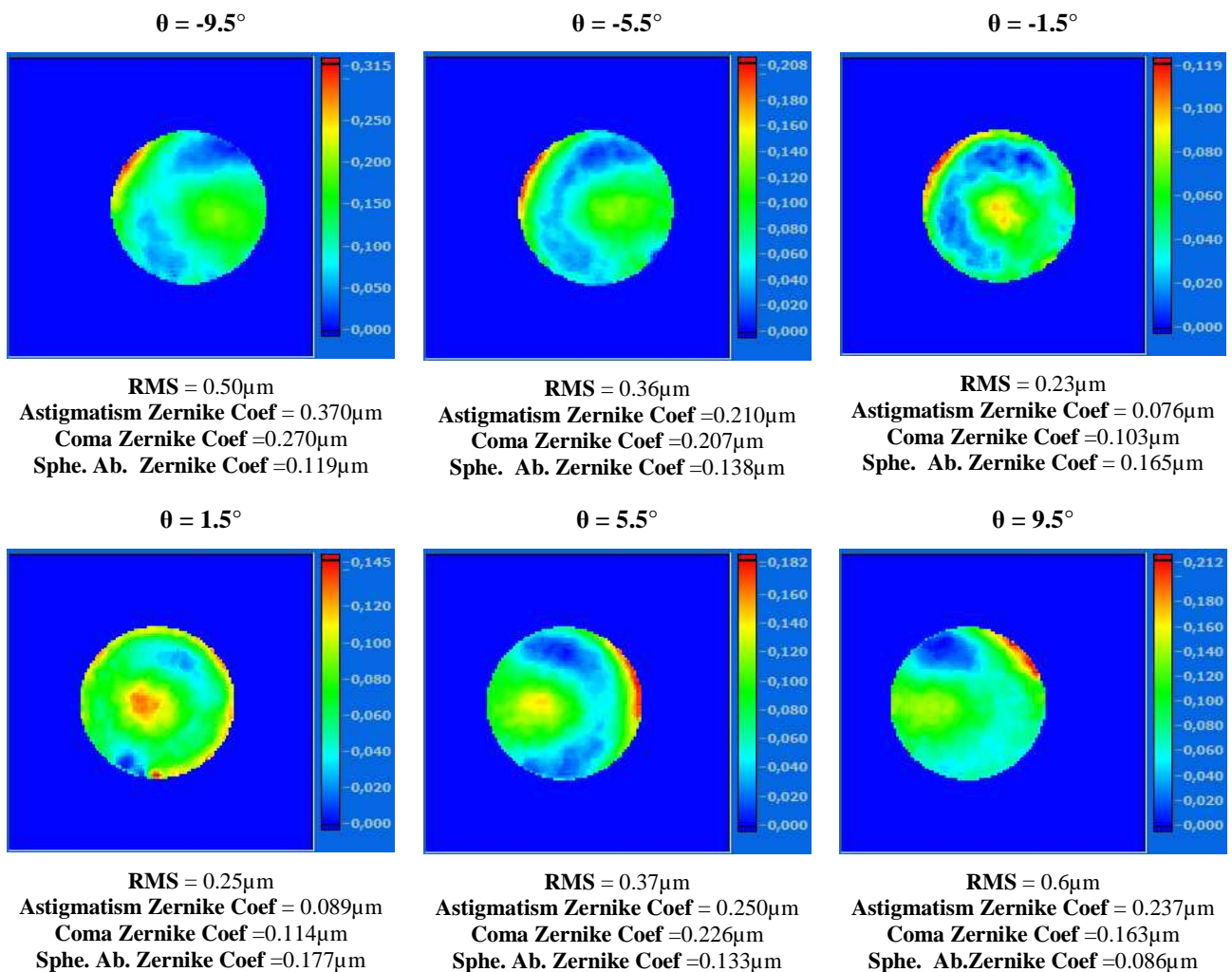


Figure 10 : Phase cartographies obtained during the field analysis ( $\theta=\pm 9.5^\circ$ ,  $\pm 5.5^\circ$  and  $\pm 1.5^\circ$ ) of the objective. The Zernike coefficients are RMS values (the phase scales are given in fraction  $\lambda$  with  $\lambda=10\mu\text{m}$ ).

#### 4. CONCLUSION

We presented the application of Quadri-Wave Lateral Shearing Interferometry (QWLSI), a wave front sensing technique, to characterize thermal infrared lenses for wavelength within 8 and 14 $\mu\text{m}$ . This technique is a powerful tool to qualify the optical quality on axis and in the field of lenses and objectives giving, in one single measurement, the cartography of the wave front but also the PSF and MTF curves. The wave front knowledge permits the detection of local defects and the PSF and MTF describe the global imaging quality of the optical system. Further developments concern first the use of CO<sub>2</sub> laser ( $\lambda=10,6\mu\text{m}$ ) as a source to make a monochromatic analysis (particularly for optical systems having chromatic aberration). We consider also the use of Quadri-Wave Lateral Shearing Interferometry in the mid wavelength infrared (MWIR) domain ( $\lambda=3-5\mu\text{m}$ ) for the metrology of objectives designed for MWIR imaging.

## REFERENCES

- [1] J. Primot and L. Sogno, "Achromatic three-wave (or more) lateral shearing interferometer," *J. Opt. Soc. Am. A* **12**, 2679-2685 (1995)
- [2] J. Chanteloup, F. Druon, M. Nantel, A. Maksimchuk, and G. Mourou, "Single-shot wave-front measurements of high-intensity ultrashort laser pulses with a three-wave interferometer," *Opt. Lett.* **23**, 621-623 (1998)
- [3] J. Primot and N. Guérineau, "Extended Hartmann Test Based on the Pseudoguiding Property of a Hartmann Mask Completed by a Phase Chessboard," *Appl. Opt.* **39**, 5715-5720 (2000)
- [4] S. Velghe, R. Haïdar, N. Guérineau, M. Tauvy, S. Rommeluère, S. Théas, G. Dunet, and J. Primot, "*In situ* optical testing of infrared lenses for high-performance cameras," *Appl. Opt.* **45**, 5903-5909 (2006)
- [5] M. Born and E. Wolf, *Principles of Optics*, Cambridge University Press, 2002, p 528